



ELSEVIER

Available online at [www.sciencedirect.com](http://www.sciencedirect.com)

SCIENCE @ DIRECT®

Journal of volcanology  
and geothermal research

Journal of Volcanology and Geothermal Research 128 (2003) 327–339

[www.elsevier.com/locate/jvolgeores](http://www.elsevier.com/locate/jvolgeores)

# Relocation of seismicity preceding the 1984 eruption of Mauna Loa Volcano, Hawaii: Delineation of a possible failed rift

Shirley Baher\*, Clifford Thurber, Kyle Roberts, Charlotte Rowe<sup>1</sup>

*Department of Geology and Geophysics, University of Wisconsin–Madison, Madison, WI 53706, USA*

Received 2 October 2002; accepted 11 June 2003

## Abstract

Waveform cross-correlation based repicking of *P* arrival times and subsequent relocation of 187 earthquakes that occurred near the summit of Mauna Loa, Hawaii, prior to the March 1984 eruption has illuminated a previously obscured structure beneath the northwestern flank. Simultaneous inversion for hypocenters and velocity model parameters using the refined arrival times resulted in well-constrained relative earthquake locations with very low arrival time misfits (average RMS 0.041 s). Pre-eruption seismicity from this time period occurred in two groups: a shallow group located near Mauna Loa's summit, at depths of 1–3 km, and a deeper group (5–10 km) located 4–6 km northwest of the summit. After relocation, we found that most of the northwest flank earthquakes occurred along a 3-km-long planar feature striking about 60° West of North in a thin band about 1 km thick. There is a temporal migration of epicenters from the northwestern edge of the zone migrating towards the summit. Focal mechanisms in this zone reveal a change in faulting from strike-slip in the southeast to a mix of strike-slip and normal faulting in the northwest. This feature we interpret to be related to a rift zone that was stunted by the buttressing of the adjacent volcanoes Hualalai and Mauna Kea. Previous gravity and magnetic studies provide supporting evidence for the existence of a rift zone. There was only a modest increase in clustering of the summit events. After relocation, hypocenters that were previously located within a diffuse zone (4.5 km) were reduced to a 2.5-km-wide zone. They extend from a depth of 6 km to about sea level, trending toward the summit. The focal mechanisms from the summit events are mix of faulting types without a consistent pattern.

© 2003 Elsevier B.V. All rights reserved.

*Keywords:* Mauna Loa; volcanoes; swarms; focal mechanisms; data processing; arrival time

## 1. Introduction

The island of Hawaii is made up of five coalesced volcanoes: Kohala, Mauna Kea, Hualalai, Mauna Loa, and Kilauea (Fig. 1a). Mauna Loa is the world's largest active volcano, covering over half of the surface area of the island of Hawaii (> 5000 km<sup>2</sup>). It has erupted over 30 times since

<sup>1</sup> Present address: Los Alamos National Laboratory, Los Alamos, NM 87545, USA.

\* Corresponding author. Present address: U.S. Geological Survey, Menlo Park, CA 94025, USA.

*E-mail address:* [sbaher@usgs.gov](mailto:sbaher@usgs.gov) (S. Baher).

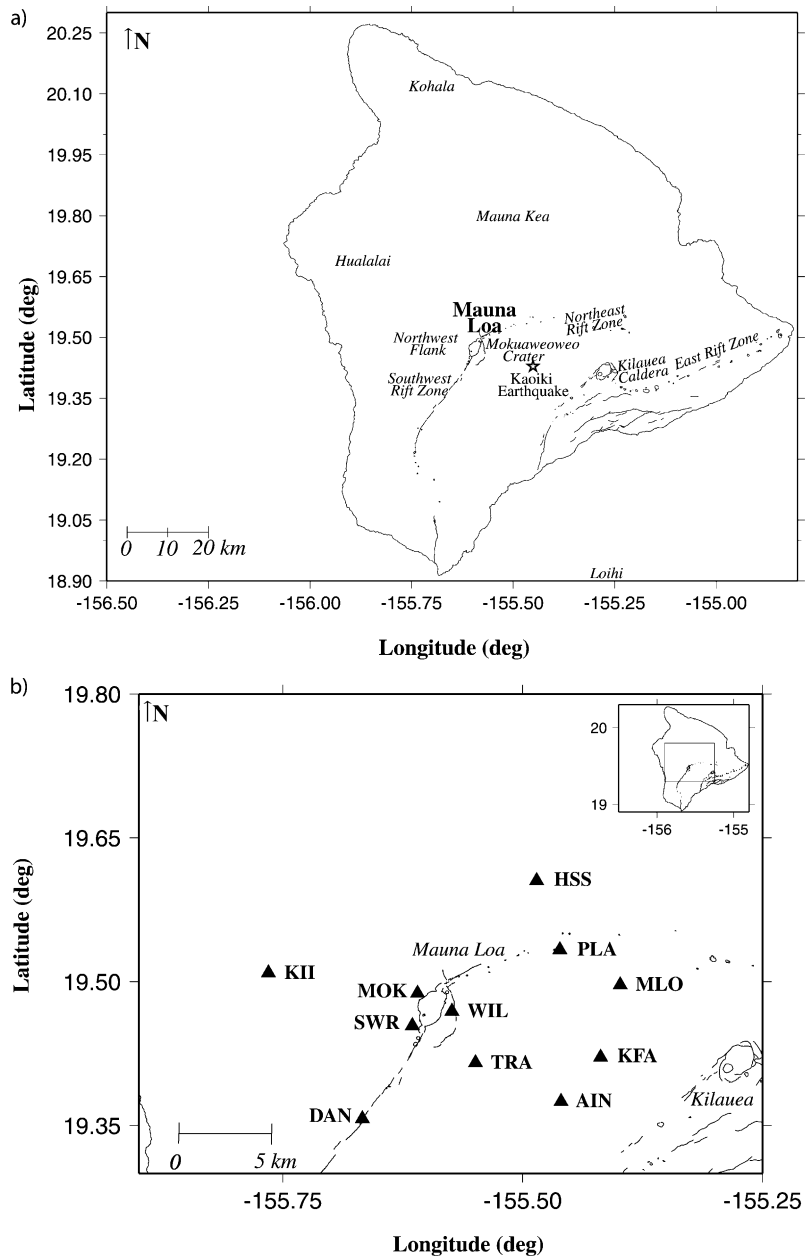


Fig. 1. (a). Map of the island of Hawaii showing the five existing volcanoes Kohala, Hualalai, Mauna Kea, Mauna Loa, and Kilauea, and the seamount Loihi. Features of Mauna Loa include the Southwest and Northeast Rift Zones, northwest flank, Mokuaweoweo crater and the Kaoiki area. (b) Station locations for the data used in this study.

its first well-documented historical eruption in 1843.

The most recent eruption at Mauna Loa occurred in March 1984. The shallow depth (< 5

km) pre-eruption seismicity steadily increased beginning from March 1982, with a marked increase beginning early March 1984 (Lockwood et al., 1985, 1987). The intermediate depth (5–13 km)

pre-eruption seismicity occurred at a more uniform rate, except for an earthquake swarm in September 1983 that activated the region to the northwest of the caldera. First motion analyses suggest that these September earthquakes resulted from increasing lateral stresses generated in the summit and upper Southwest Rift Zone possibly from an intrusion of magma (Lockwood et al., 1985, 1987). Also relevant to the pre-eruption seismicity is the 16 November 1983 ( $M=6.6$ ) earthquake in the Kaoiki region (Fig. 1a), which is on the southeast flank of Mauna Loa. Following this earthquake, the number of deeper (5–13-km) summit events increased, and the seismically active zone extended from the southwest flank into the northeast rift zone (Okubo, 1995). Since the 1984 eruption, Mauna Loa has been in repose.

The preceding July 1975 eruption of Mauna Loa followed 25 years of repose after the large Southwest Rift Zone eruption of June 1950. Decker et al. (1983) and Lockwood et al. (1985, 1987) noted similarities between the pre-1975 and pre-1984 pre-eruption seismicity patterns. For both eruptions, the seismicity was concentrated in the regions to the northwest and near the summit of Mokuaweoweo crater. Pre-eruption flank seismicity has also been recorded at several other volcanoes (e.g. Miyake–Jima, Japan (Minakami, 1974); Kilauea, Hawaii (Gillard et al., 1992; Klein et al., 1987); Unzen, Japan (Ohta et al., 1992); Mt. Pinatubo, the Philippines (Harlow et al., 1996; Jones et al., 2001); Mt. Etna, Italy (Bonaccorso and Patane, 2001)). The Hawaiian Volcano Observatory in their 1983 summary report (Nakata et al., 1983) stated that based on the similarity in the pattern of Mauna Loa earthquakes and deformation in 1983 compared to 1974 (the year prior to the July 1975 eruption), they were prompted to issue a statement indicating a higher than average probability of an eruption in 1984.

Waveform cross-correlation techniques used to improve earthquake locations have shown success in better delineating volcanic subsurface structures (e.g. Gillard et al., 1996; Rubin et al., 1998; Jones et al., 2001; Zollo et al., 2001), and in defining magmatic processes (e.g. Aspinall et al., 1998; Kauahikaua, 1993). These studies pro-

vide new insights into assessing the relationship between seismicity and magmatic activity, and have given a clearer understanding of the seismically active structures within a volcano. Previous analyses of Kilauea's rift zones in particular can assist in the understanding of Mauna Loa. From an analysis of Kilauea Upper East Rift zone earthquakes, Gillard et al. (1996) identified a narrow band of shallow seismicity that they proposed was generated by the widening of the underlying deep rift zone. An analysis of Kilauea's Middle East Rift Zone seismicity by Rubin et al. (1998) found a similar pattern of concentrated activity. The authors concluded that the narrow bands of seismicity were consistent with growing stress concentrations above a deforming deeper magma body. Here we apply waveform cross-correlation in an effort to sharpen the pattern of seismicity prior to Mauna Loa's 1984 eruption.

## 2. Data processing

Earthquakes analyzed in this study were from Mauna Loa's pre-eruption activity (April 1983–April 1984) recorded at the Hawaiian Volcano Observatory (Nakata et al., 1983; Nakata et al., 1984), and were selected on the basis of their catalog locations and magnitudes. We examined in detail 187 events located on the northwest flank of the Mauna Loa and near the summit with amplitude magnitudes equal to or exceeding 1.1 and hypocentral depths <12 km. Note that only a small number of low-magnitude events with very few observations were excluded from our analysis, so we consider this set to provide a relatively complete picture of the pre-eruption seismicity. The selected events were recorded on at least 6 of the 11 stations surrounding the Mokuaweoweo crater (Fig. 1b). The data were from 1-Hz geophones recorded at 100 samples per second.

Upon visual examination of the waveforms, we observed a high degree of waveform similarity. This led us to apply waveform cross-correlation methods to improve phase pick consistency (e.g. Fremont and Malone, 1987; VanDecar and Crosson, 1990; Dodge et al., 1995; Shearer,

1997; Shearer, 1998; Aster and Rowe, 2000; Rowe, 2000; Rowe et al., 2002a,b). We used a method following the approach of Dodge et al. (1995) and others, which simultaneously analyzes events on a station-by-station basis to capitalize on consistency of wave source and propagation effects, rather than examining traces across all stations on an event-by-event basis. The best constraints on relative pick times can be expected to be found between the most similar earthquake waveforms, which arise from events with the most consistent radiation patterns, moment rate functions and propagation paths (Rowe et al., 2002a).

The initial step of repicking of the  $P$  arrivals is to manually estimate the arrival times and assign a pick quality rating based on an analyst estimate of pick accuracy and signal to noise ratio. High confidence picks, with high signal to noise ratio (3:1) and a pick uncertainty of less than 0.05 s were assigned a quality rating of 0, whereas picks with low confidence, defined by a low signal to noise ratio (1.5:1) and pick uncertainty of 0.5 s were assigned a quality rating of 3. Pick uncertainties of 0.1 and 0.3 s were assigned quality ratings of 1 and 2, respectively, with uncertainties greater than 0.5 s given a quality rating of 4, and not included in this study.

Relative lag estimation between pairs of traces was then determined in two steps; a coarse (discrete) correlation step and a fine (sub-sample) correlation step. A 200-sample window was established surrounding the preliminary picks for each pair of events to be compared. This allowed us to include several cycles of the waveform with data sampled at 100 samples/s. In the case of highly similar seismograms, the attainable lag resolution is significantly less than the sample interval (Poupinet et al., 1984). This level of precision is desirable to accurately image fault structures, which may have spatial scales of tens of meters or less.

The clustering used for this analysis was based on the values of the single-station cross-correlation (Rowe et al., 2002a). Initial clustering was performed using master station PLA, which was chosen based on its high quality of data and off-summit location. Not all the traces were included

with clusters. We chose to include the remaining ‘orphan’ traces if they were determined to be of high quality, exhibiting high signal to noise ( $\geq 3:1$ ) and a low pick uncertainty ( $< 0.05$  s).

After single-station clustering, intra-cluster cross-correlation was performed using a suite of correlation window lengths. All traces within a cluster were cross-correlated for each of the window lengths. After several trials, the optimum lags were determined and pick adjustments were made for all events within a cluster (Fig. 2). The event clustering for the remaining stations was based on the clusters established for PLA. The pick adjustments were made for the remaining stations based on the method described above.

To further refine the picks, waveforms within each cluster were aligned on their adjusted picks and stacked. Each stack was then treated as a composite earthquake trace for that cluster. Ensembles of stacked seismograms were then cross-correlated and the relative pick lags were determined. The resulting inter-cluster lags were then used to adjust mean picks within each cluster. This method preserves the very tightly constrained relative adjustments for intra-cluster associations, with no risk of degrading these relative adjustments by mistakenly including uncorrelated events through preliminary mislocation or introducing analyst pick bias.

### 3. Earthquake relocation procedure

We next determined more precise locations for the earthquakes preceding the 1984 Mauna Loa eruption by utilizing the adjusted  $P$  arrival picks for joint hypocenter determination (JHD). The results of a preliminary 1-D JHD inversion using the algorithm VELEST (Kissling et al., 1994) showed a lineation in the structure on the northwest flank and a slight increase in clustering of seismicity in the near-summit events. The quality of the VELEST results was poorer than expected, however, possibly due to the large range in station elevations (nearly 4 km), when VELEST assumes all stations are on a plane. Since the range of depths for the events used in this study is from  $-1.5$  to 10 km (relative to sea level), and station

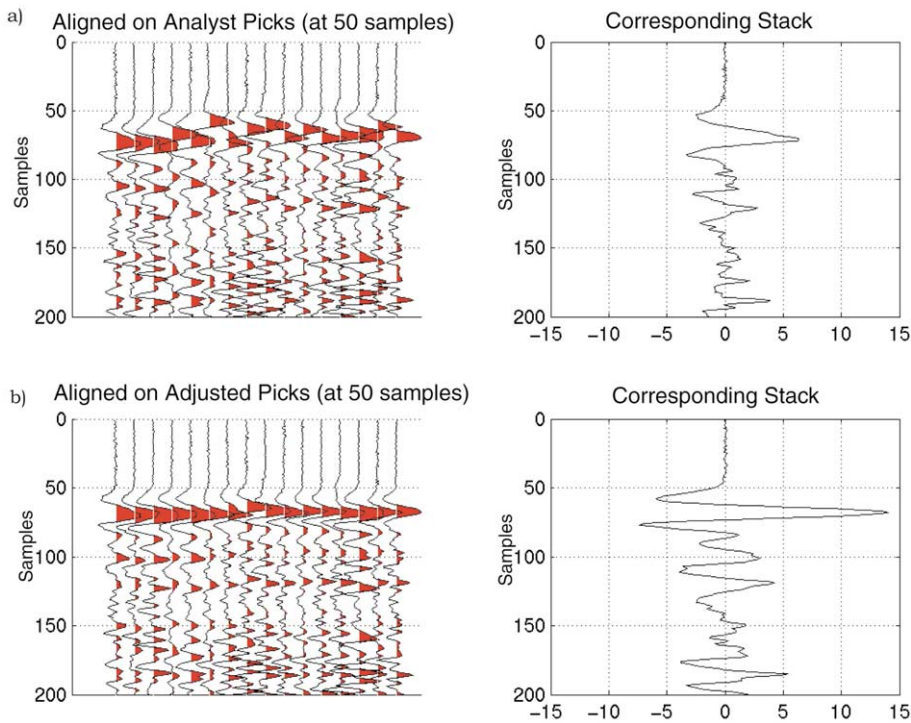


Fig. 2. (a). Plot showing initial analyst picks and the corresponding waveform stack ( $P$  wave first arrivals aligned at 50 samples; sample rate is 100 samples/s). (b) Adjusted picks after waveform cross-correlation and the corresponding stack.

elevations range from near sea level to over 4 km, we concluded that event relocation with a more sophisticated algorithm was necessary. Therefore, starting with the 1-D velocity model generated from VELEST, a subsequent 1-D inversion was performed with a code allowing for true station elevations, simul2000 (Thurber and Eberhart-Phillips, 1999). The nodes of the simul2000 velocity model were based on the VELEST layering, at depth intervals ranging from 1.2 km near the surface increasing to 5.5 km at 15 km depth (Fig. 3).

The initial simul2000 inversion with the refined  $P$  arrival picks was able to resolve a subhorizontal linear feature beneath the northwest flank of Mauna Loa. There was also an increase in clustering of seismicity for the near-summit events, but no clear features were resolved. We observed, however, that the RMS residuals ranged between 0.01 and 0.16 s, with an average RMS of 0.041 s. An examination of the pattern of residuals revealed that the high RMS values were for the near-summit events, while the RMS values for

the northwest flank events were no greater than 0.05 s.

Due to the lateral heterogeneity of our study area, there was a concern that the use of a 1-D velocity model was insufficient to describe the entire region, causing the high RMS values for the near-summit events. At the same time, the dataset was judged not to be suitable for a full 3-D inversion. To resolve this issue, we separated the events into two distinct groups (near-summit and northwest flank) in order to try to improve the RMS values. The same starting velocity model was used for the inversion for each of the event groups. The RMS was reduced for the near-summit group from  $\leq 0.16$  s to  $< 0.05$  s, while keeping northwest flank group's RMS consistent with the initial inversion. The resulting average uncertainties in relative locations for the northwest flank group's events were 0.10 km, 0.11 km, and 0.18 km, and for the summit events they were 0.12 km, 0.11 km, 0.29 km for the  $x$ ,  $y$ , and  $z$  directions, respectively. As a result of the

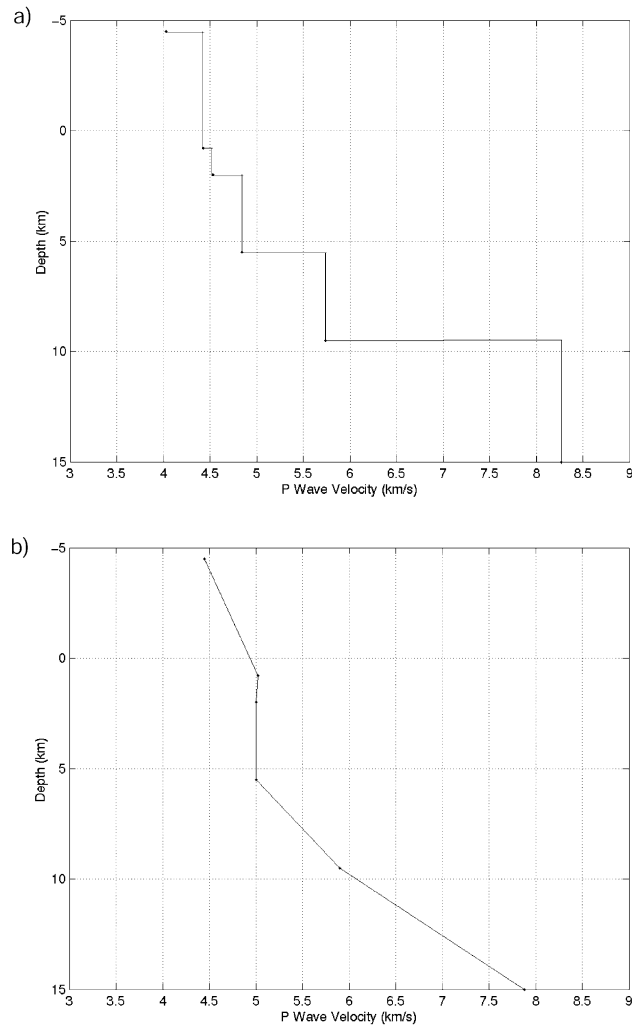


Fig. 3. (a) Velocity model used as input to VELEST. (b) Velocity model used as input to simul2000.

improvement in the RMS residuals, the analysis of relocated events is based on the regionally grouped events.

#### 4. Fault plane solutions

Focal mechanisms were generated using the FPFIT algorithm (Reasenberg and Oppenheimer, 1985) for all events. The focal mechanisms from the northwest flank showed a change in faulting from strike-slip in the southeast segment to a variety of mechanisms in the northwest segment and

normal faulting in the transition zone in between the two segments. The near-summit events show a variety of focal mechanisms without any predominant pattern.

Assuming a double couple fault plane solution, focal mechanisms were determined using the FPFIT algorithm (Reasenberg and Oppenheimer, 1985). The majority of the events in this study had a misfit score in the range 0.0–0.25, indicating high consistency, with only 2% of the events in the 0.175–0.200 range. After rechecking the polarity data of the discrepant focal mechanisms, they were recomputed if necessary.

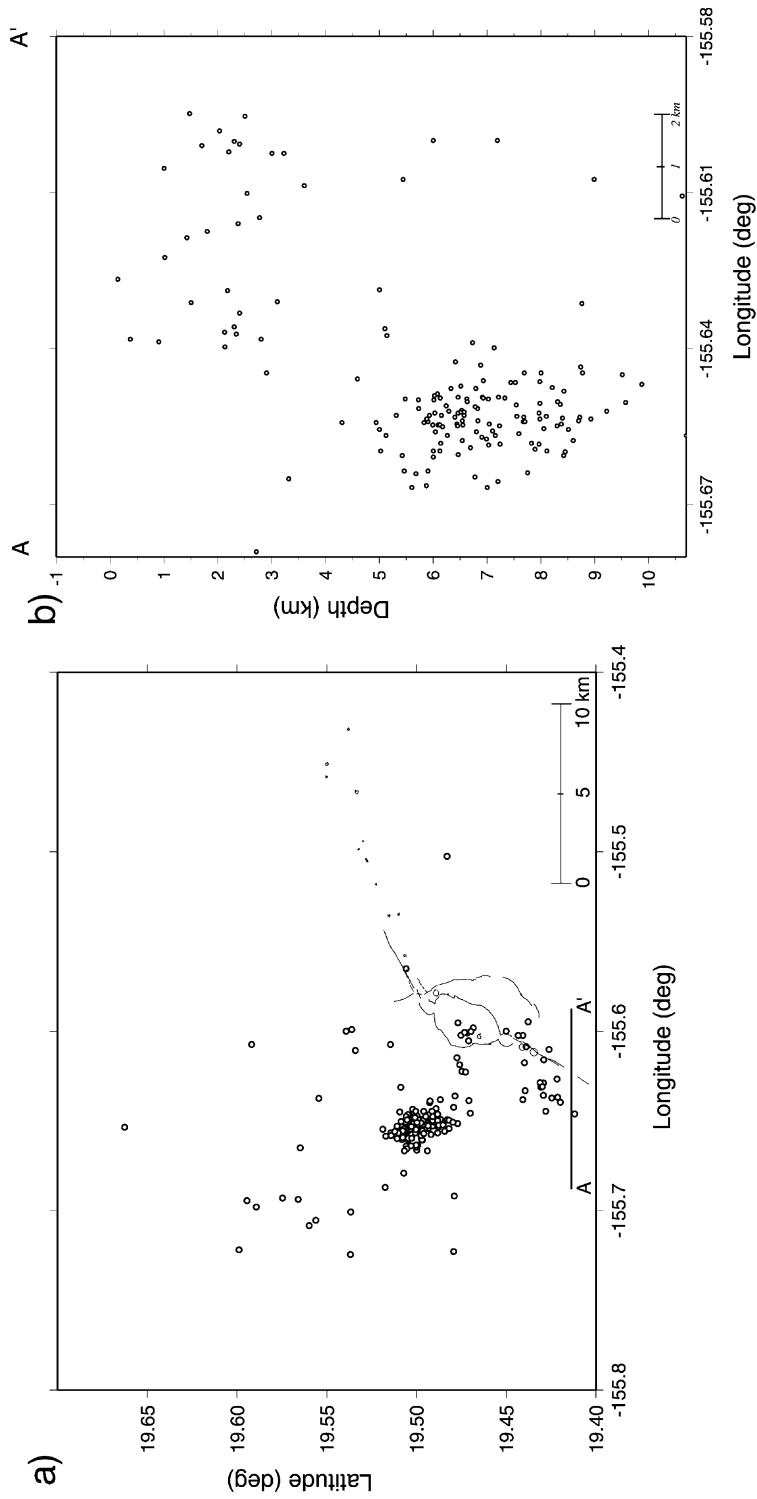


Fig. 4. (a) Map view and (b) depth section of the catalog locations for the pre-1984 eruption events.

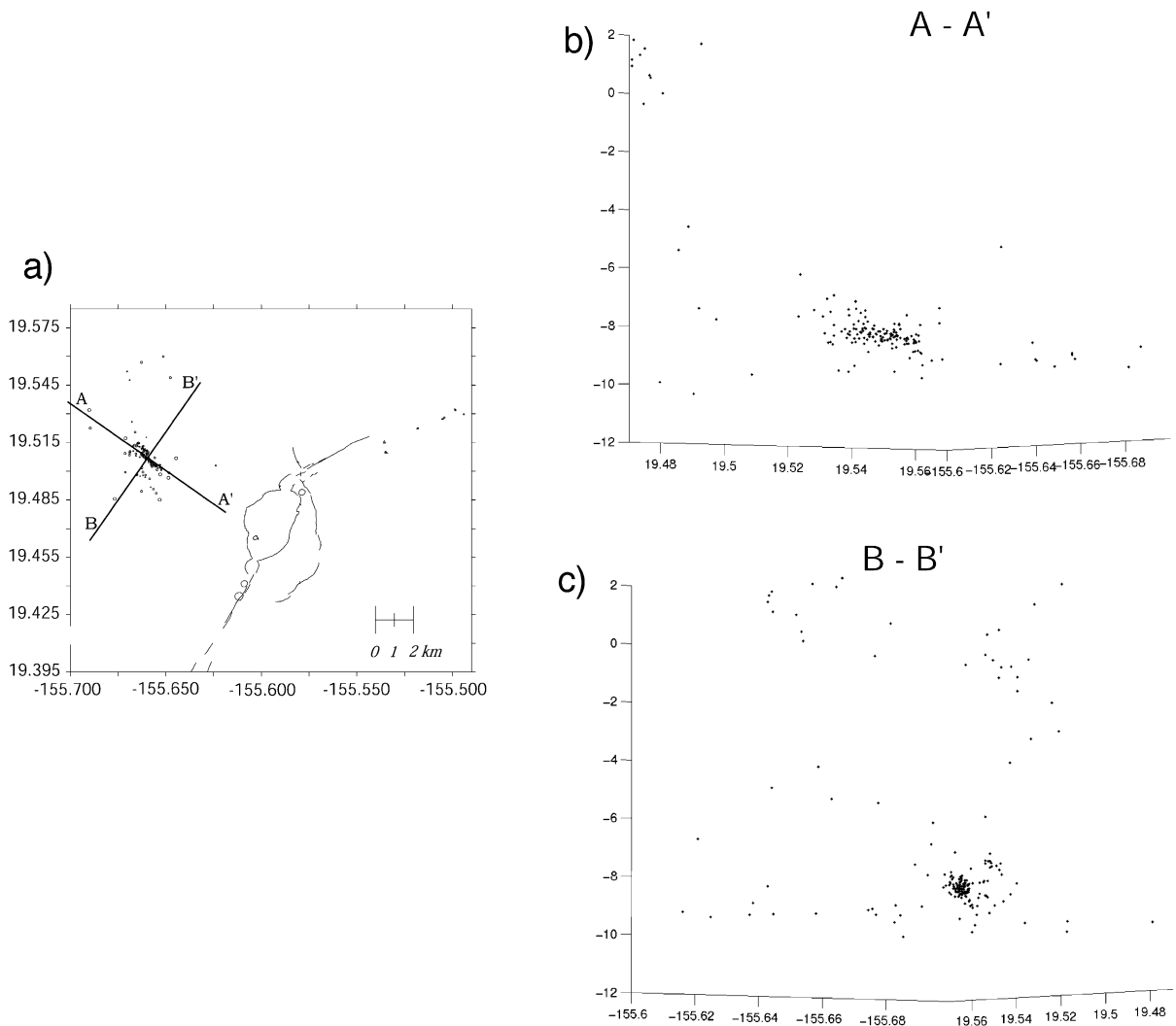


Fig. 5. Relocated seismicity for the northwest flank cluster. (a) Map view of the relocated events. (b) Depth section A–A' oriented 125° clockwise from north. (c) Depth section B–B' oriented 215° clockwise from north.

## 5. Results

Hypocenters were relocated from beneath the northwest flank and the near-summit region of Mauna Loa volcano. The catalog hypocenter locations beneath the northwest flank form a 3-km-high cloud at an average depth of 6.5 km (Fig. 4). In contrast, the relocated hypocenters are concentrated 4–6 km NW from the summit along a 2–3-km-long planar feature striking approximately 60° West of North in a thin band (about 1 km thick) at an average depth of 8 km (Fig. 5). There was

also a slight increase in the clustering of the seismicity for the near-summit events, as evidenced by a decrease in the lateral extent of the hypocenters compared to the catalog location from 4.5 to 2.5 km (Fig. 6). In depth section, the relocated hypocenters trace out a narrower band extending from a depth of 6 km towards the surface near the summit.

The cluster of northwest flank events shows evidence of a temporal migration towards the summit. The initial events from the September 1983 swarm were located beneath the flank at

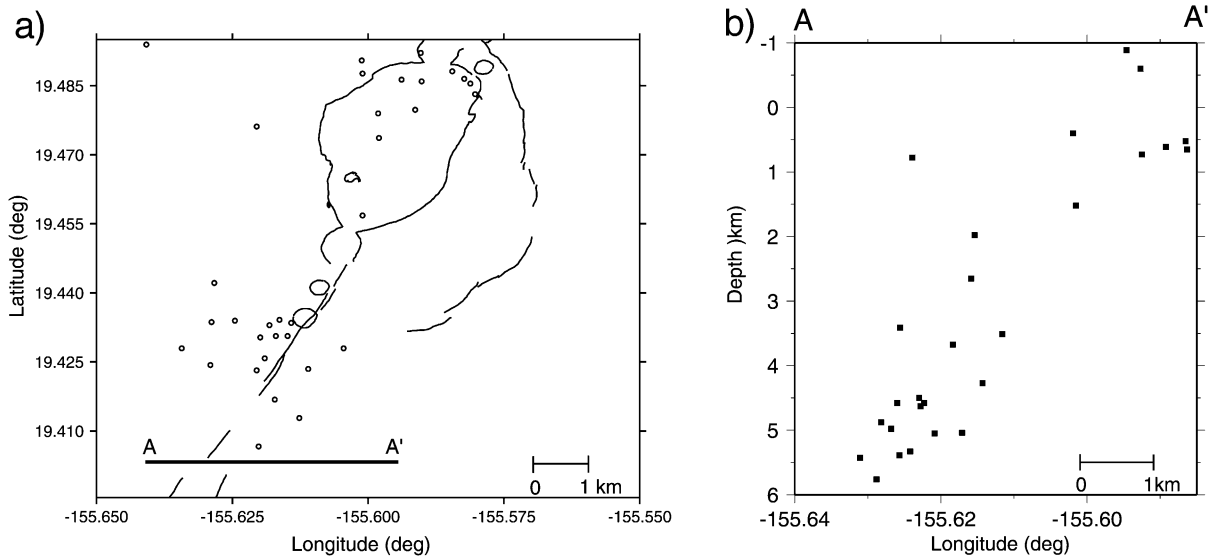


Fig. 6. (a) Map view and (b) depth section for the relocated near-summit events.

the northwest end of the cluster ( $19^{\circ}51'N$ ,  $155^{\circ}66'W$ ) with the later events located nearer the summit ( $19^{\circ}50'N$ ,  $155^{\circ}65'W$ ). We did not observe any temporal migration of epicenters within the near-summit group of events.

Focal mechanisms beneath the northwest flank show a change in faulting from strike-slip in the southeast to normal faulting (dip-slip) and mixed (strike-slip, dip-slip) in the northwest (Fig. 7a). The mechanisms are generally consistent with East–West extension. When we compare the faulting mechanisms with the time migration of epicenters, the initial events show mixed faulting and then evolve into strike-slip motion. There are several possible reasons for this change, including the fracture of the subsurface structure as a result of a dike intrusion (Dominguez et al., 2001; Bonaccorso and Patane, 2001) or the effects of a regional stress field. Previous analysis of the regional stresses on the west side of Mauna Loa shows seaward motion as a result of basal slip at about 12 km depth (Bryan and Johnson, 1991). Gillard et al.'s (1992) analysis of focal mechanisms at Mauna Loa found evidence of a mixture of dip-slip and strike-slip faulting, with an axis of least compressive stress to be oriented roughly East–West, consistent with our mechanisms.

Near-summit focal mechanisms show a variety of strike-slip and dip-slip focal mechanisms (Fig. 7b). Thurber (1987) also observed an apparent random pattern of near-summit focal mechanisms at Kilauea volcano and suggested the possibility that there was a change in stress orientation related to a shift in direction of magmatic activity. Prior to the 1991 eruption at Mt. Pinatubo, focal mechanisms for the near-summit cluster were also highly mixed (Bautista et al., 1996). They concluded that this was the result of a magmatic intrusion. The combination of strike-slip and subsequent dip-slip mechanisms, as shown in these studies, may be the result of a combination of tectonic and magmatic activity.

## 6. Discussion

The 1975 and 1984 eruptive sequences provided opportunities to observe and analyze many aspects of Mauna Loa's seismic activity. The repeatability of a flank followed by summit sequence that occurred both during 1975 and 1984 leads us to conclude that they were directly related to volcanic processes and crustal deformation induced by volcanism. Eruptions and related seismic activity normally occur at the summit or ei-

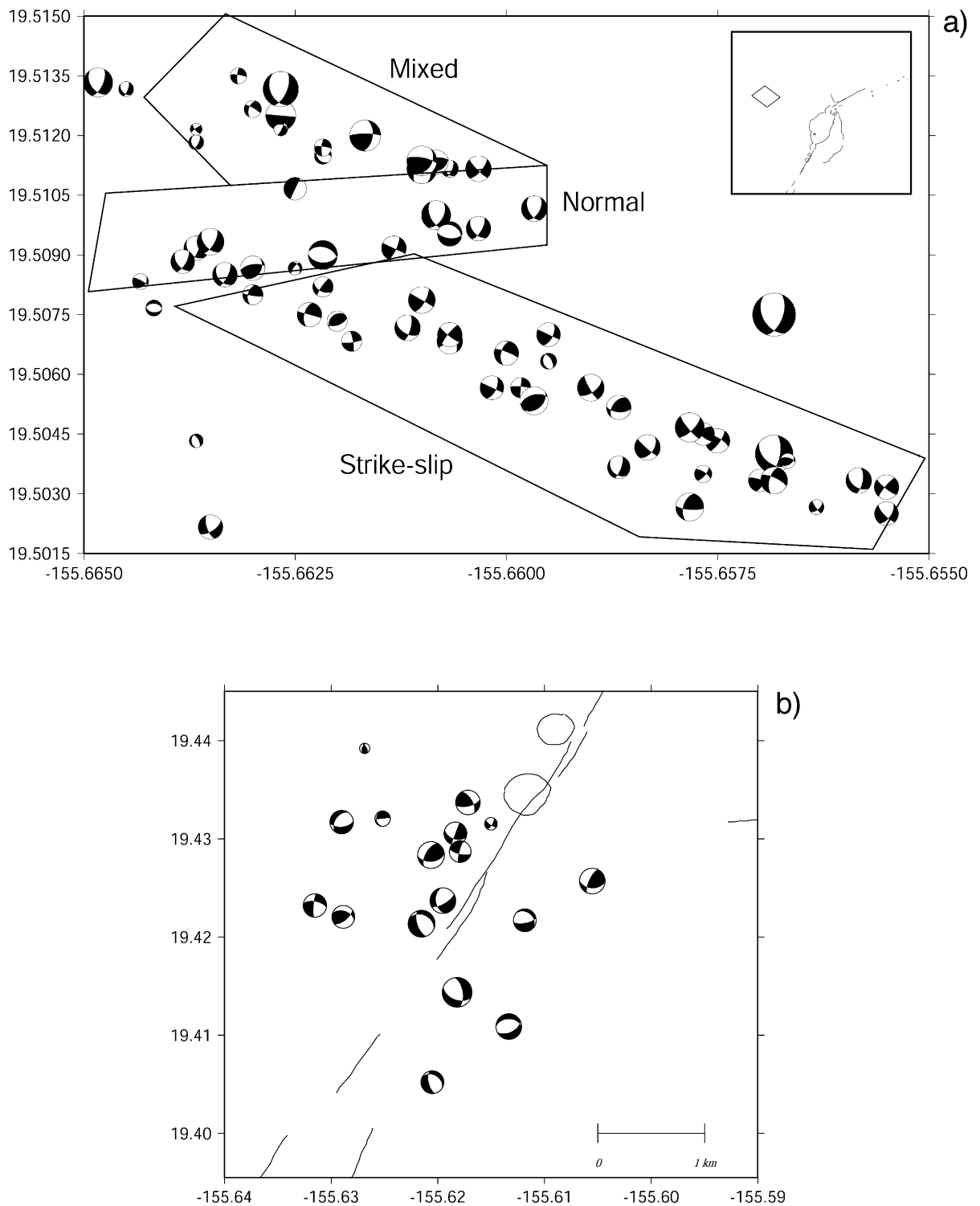


Fig. 7. (a) Focal mechanisms for the events beneath the northwest flank. (b) Focal mechanisms for the near-summit events.

ther rift zones, so it is the flank activity that requires an explanation.

Much of the off-summit volcanic activity in Hawaii takes place along linear rift zones that radiate from the main volcanic centers. Such rift zones, located on oceanic seamounts or islands like Hawaii, generally develop in a characteristic triple arm or ‘stellate’ geometry that tends to become more pronounced throughout the life of the edifice (Fiske and Jackson, 1972; Carracedo, 1994). The main process by which these geometries are achieved is thought to be the ‘least effort’ fracturing produced by magma-induced unloading (Luongo et al., 1991). The original ‘stellate’ character of this regular geometry of the rift zones is often lost due to gravitational forces and the buttressing of existing topographic features, such as adjacent volcanoes (Carracedo, 1999). When rifts are poorly developed, eruptions tend to take place from vents radiating in all directions from the summit (Carracedo, 1996); this is evidenced on Mauna Loa’s northwest flank (Lipman, 1995).

According to Fiske and Jackson (1972), the rift zones at Mauna Kea initially developed in the triple arm geometry (Fig. 8a). Its third arm started to develop directly opposite to the southeast and northeast rift zones but was stunted due to the topographic expression of the Kohala and Hualalai volcanoes. Similarly, the northwest flank cluster of hypocenters at Mauna Loa could represent a poorly developed or failed rift that has been stunted by the buttressing of adjacent volcanoes Hualalai and Mauna Kea (Fig. 8a).

Gravity field variations are a useful tool for studying the magmatic plumbing system of Hawaii’s volcanoes, because the rift cores are systematically denser than extrusive flows. Krivoy and Eaton (1961) and Kinoshita et al. (1963) published the first gravity maps of the island of Hawaii. Kauahikaua et al. (2000) recently analyzed over 3300 gravity measurements taken on the island of Hawaii. Their modeling of Mauna Loa’s northwest flank shows a positive anomaly extending linearly outward to the northwest from the summit with no surface evidence of a rift zone. Hawaii’s topographic contours (Fig. 8a) also show a knee near our proposed rift zone.

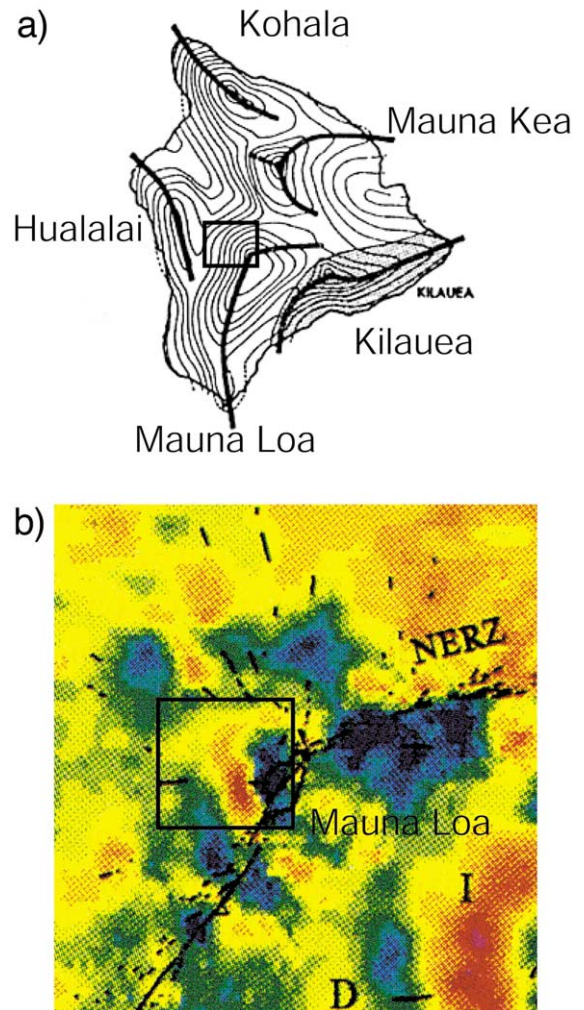


Fig. 8. (a) Map of topographic contours and rift locations for the island of Hawaii (adapted from Fiske and Jackson (1972)). (b) Portion of the map of magnetic anomalies of Hawaii in the vicinity of Mauna Loa (adapted from Hildenbrand et al., 1993).

When the initial aeromagnetic map of the island of Hawaii was developed by Malahoff and Woollard (1966), they discovered that magnetic anomalies correlated with central vent areas and rift zones. It is recognized that a characteristic rift zone pattern is a high–low anomaly (Hildenbrand et al., 1993). Such a pattern is observed on the northwest flank near our proposed failed rift zone (Fig. 8b).

## 7. Conclusions

Waveform cross-correlation based repicking of *P* arrival times and relocation of earthquakes improved the relative locations for the selected pre-1984 eruption events at Mauna Loa volcano. During the September 1983 swarm, most of the seismic activity beneath the northwest flank occurred along a planar feature, which may be related to a failed rift zone that becomes activated prior to eruptions. The summit activity showed an increase in clustering after relocation, but no clear structural features emerged. Results of previously analyzed gravity data (Kauahikaua et al., 2000) revealed an increase in gravity along a line radiating out from the summit, near the relocated northwest flank events. Previous analysis of magnetic data (Hildenbrand et al., 1993) shows a characteristic rift high–low anomaly beneath the northwest flank. Thus the available geophysical evidence presents consistent support for a subsurface structure extending radially to the northwest from the summit, which we propose is a failed rift zone.

## Acknowledgements

We thank Paul Okubo of the Hawaiian Volcano Observatory for providing access to the data. We are grateful to Allan Rubin and Steve Malone for their constructive comments on the manuscript. We also acknowledge the help of Joshua Jones on initial data collection and analysis, and that by William Lutter for data processing assistance. This material is based upon work supported by the National Science Foundation under Grant No. EAR-0001138.

## References

- Aspinall, W.P., Miller, A., Lynch, L., Latchman, J., Stewart, R., White, R., Power, J., 1998. Soufriere Hills eruption, Montserrat, 1995–1997: Volcanic earthquake locations and fault plane solutions. *Geophys. Res. Lett.* 25, 3397–3400.
- Aster, R.C., Rowe, C.A., 2000. Automatic phase pick refinement and similar event association in large seismic datasets. In: Thurber, C., Rabinowitz, N. (Eds.), *Advances in Seismic Event Location*. Kluwer, Dordrecht, pp. 231–263.
- Bautista, B.C., Bautista, M., Stein, R., Barcelona, E., Punongbayan, R., Laguerta, E., Rassdas, A., Ambubuyog, G., Amin, E., 1996. Relationship of regional and local structures to Mount Pinatubo activity. In: Newhall, C.G., Punongbayan, R.S. (Eds.), *Fire and Mud: Eruptions and Lahars of Mount Pinatubo, Philippines*. PHIVOLCS, Quezon City, University of Washington Press, Seattle, WA, pp. 351–370.
- Bonaccorso, A., Patane, D., 2001. Shear response to an intrusive episode at Mt. Etna volcano (January, 1988) inferred through seismic and tilt data. *Tectonophysics* 334, 61–75.
- Bryan, J.D., Johnson, C.E., 1991. Block tectonics of the island of Hawaii from focal mechanism analysis of basal slip. *Bull. Seismol. Soc. Am.* 81, 491–507.
- Carracedo, J.C., 1994. The Canary Islands: An example of structural control on the growth of large oceanic-island volcanoes. *J. Volcanol. Geotherm. Res.* 60, 225–241.
- Carracedo, J.C., 1996. Morphological and structural evolution of the western Canary Islands: Hotspot-induced three-armed rifts or regional tectonic trends? *J. Volcanol. Geotherm. Res.* 72, 151–162.
- Carracedo, J.C., 1999. Growth, structure, instability and collapse of Canarian volcanoes and comparisons with Hawaiian volcanoes. *J. Volcanol. Geotherm. Res.* 94, 1–19.
- Decker, R.W., Koyanagi, R.Y., Dvorak, J.J., Lockwood, J.P., Okamura, A.T., Yamashita, K.M., Tanigawa, W.R., 1983. Seismicity and surface deformation at Mauna Loa volcano, Hawaii. *Eos Trans. AGU* 64, 545–547.
- Dodge, D.A., Beroza, G., Ellsworth, W., 1995. Evolution of the 1992 Landers, California foreshock sequence and its implications for earthquake nucleation. *J. Geophys. Res.* 100, 9865–9980.
- Dominguez, T., Zobin, V.M., Reyes-Davila, G.A., 2001. The fracturing in volcanic edifice before an eruption: The June–July 1998 high-frequency earthquake swarm at Volcan de Colima, Mexico. *J. Volcanol. Geotherm. Res.* 105, 65–75.
- Fiske, R.S., Jackson, E.D., 1972. Orientation and growth of Hawaiian volcanic rifts: The effect of regional structure and gravitational stress. *Proc. R. Soc. Lond. (A)* 329, 299–320.
- Fremont, M.J., Malone, S., 1987. High precision relative locations of earthquakes at Mount St. Helens, Washington. *J. Geophys. Res.* 92, 10223–10236.
- Gillard, D., Wyss, M., Nakata, J., 1992. A seismotectonic model for western Hawaii based on stress tensor inversion from fault plane solutions. *J. Geophys. Res.* 97, 6629–6641.
- Gillard, D., Rubin, A., Okubo, P., 1996. Highly concentrated seismicity caused by deformation of Kilauea's deep magma system. *Nature* 384, 343–346.
- Harlow, D.H., Power, J.A., Laguerta, E.P., Ambubuyog, G., White, R.A., Hoblitt, R.P., 1996. Precursory seismicity and forecasting of the June 15, 1991, eruption of Mount Pinatubo. Newhall, C.G., Punongbayan, R.S. (Eds.), *Fire and Mud: Eruptions and Lahars of Mount Pinatubo, Philippines*. PHIVOLCS, Quezon City, Univ. of Washington Press, Seattle, WA, pp. 285–305.
- Hildenbrand, T.G., Rosendbaum, J.G., Kauahihaua, J.P.,

1993. Aeromagnetic study of the Island of Hawaii. *J. Geophys. Res.* 98, 4099–4119.
- Jones, J.P., Thurber, C.H., Lutter, W.J., 2001. High-precision location of pre-eruption seismicity at Mount Pinatubo, Philippines, 30 May–3 June 1991. *Phys. Earth Planet. Inter.* 123, 221–232.
- Kauahikaua, J., 1993. Geophysical characteristics of the hydrothermal systems of Kilauea Volcano, Hawaii. *Geothermics* 22, 271–299.
- Kauahikaua, J., Hildenbrand, T., Webbing, M., 2000. Deep magmatic structures of Hawaiian volcanoes imaged by three-dimensional gravity models. *Geology* 28, 883–886.
- Kissling, E., Ellsworth, W., Eberhart-Phillips, D., Kradolfer, U., 1994. Initial reference models in local earthquake tomography. *J. Geophys. Res.* 99, 19635–19646.
- Klein, F.W., Koyanagi, R.Y., Nakata, J.S., Tanigawa, W.R., 1987. The seismicity of Kilauea's magma system. *U.S. Geol. Surv. Prof. Pap.* 1350, 1019–1187.
- Kinoshita, W.T., Krivoy, H.L., Mabey, D.R., Macdonald, R.R., 1963. Gravity survey of the island of Hawaii. *U.S. Geol. Surv. Prof. Pap.* 475-C, C114–C116.
- Krivoy, H.L., Eaton, J.P., 1961. Preliminary gravity survey of Kilauea Volcano, Hawaii. *U.S. Geol. Surv. Prof. Pap.* 424-D, D205–D208.
- Lipman, P.W., 1995. Declining growth of Mauna Loa during the last 100,000 years: Rates of lava accumulation vs. gravitational subsidence. In: Rhodes, J.M., Lockwood, J.P. (Eds.), *Mauna Loa Revealed – Structure, Composition, History, and Hazards*. American Geophysical Union, Washington DC, pp. 45–80.
- Lockwood, J.P., Banks, N.G., English, T.T., Greenland, L.P., Jackson, D.B., Johnson, D.J., Koyangi, R.Y., Mc Gee, K.A., Okamura, A.T., Rhodes, J.M., 1985. The 1984 eruption of Mauna Loa volcano, Hawaii. *Eos Trans. AGU* 66, 169–171.
- Lockwood, J.P., Dvorak, J., English, T., Koyanagi, R., Okamura, A., Summers, M., Tanigawa, W., 1987. Mauna Loa 1974–1984: A decade of intrusive and extrusive activity. In: Decker, R.W., Wright, T.L., Stauffer, P.H. (Eds.), *Volcanism in Hawaii*. U.S. Geol. Surv. Prof. Pap. 1350, pp. 537–570.
- Luongo, G., Cubellis, E., Obrizzo, F., Petrazzuoli, S.M., 1991. A physical model for the origin of volcanism of the Tyrrhenian margin: The case of the Neapolitan area. *J. Volcanol. Geotherm. Res.* 48, 173–185.
- Malahoff, A., Woollard, G.P., 1966. Magnetic surveys over the Hawaiian Islands and their geological implications. *Pac. Sci.* 20, 265–311.
- Minakami, T., 1974. Seismology of volcanoes in Japan. Civette, L., et al. (Eds.) *Physical Volcanology, Developments in Solid Earth Geophysics* 6 Elsevier, Amsterdam, pp. 1–27.
- Nakata, J.S., Timor, A.H., Kayoing, R.Y., Tanigawa, W.R., 1983. Hawaii Volcano Observatory Summary 83, Seismic Data, January to December 1983. U.S. Geol. Surv. Rep.
- Nakata, J.S., Kayoing, R.Y., Timor, A.H., Tanigawa, W.R., 1984. Hawaii Volcano Observatory Summary 84, Seismic Data, January to December 1984. U.S. Geol. Surv. Rep.
- Ohta, K., Matsuwo, N., Yanagi, T., 1992. The 1990–1992 eruption of Unzen Volcano. Yanagi, T., Okada, H., Ohta, K. (Eds.), *Unzen Volcano: The 1990–1992 Eruption*, pp. 33–37.
- Okubo, P., 1995. The seismological framework for Mauna Loa volcano, Hawaii. Rhodes, J.M., Lockwood, J.P. (Eds.), *Mauna Loa Revealed – Structure, Composition, History, and Hazards*. American Geophysical Union, Washington DC, pp. 187–197.
- Poupinet, G., Ellsworth, W.L., Frechet, J., 1984. Monitoring velocity variations in the crust using earthquake doublets: An application to the Calaveras fault, California. *J. Geophys. Res.* 89, 5719–5731.
- Reasenber, P., Oppenheimer, D., 1985. FPFIT, FPLOT, and FPPAGE: FORTRAN computer program for calculating and displaying earthquake fault plane solutions. *U.S. Geol. Surv. Open-File Rep.* 85–79.
- Rowe, C.A., 2000. Correlation-Based Pick Corrections and Similar Earthquake Family Identification in Large Seismic Waveform Catalogues. Ph.D. Thesis, New Mexico Institute of Mining and Technology.
- Rowe, C.A., Aster, R.C., Borchers, B., Young, C.J., 2002a. An automatic, adaptive algorithm for refining phase picks in large seismic data sets. *Bull. Seismol. Soc. Am.* 92, 1660–1674.
- Rowe, C.A., Aster, R.C., Phillips, W.S., Jones, R.H., Borchers, B., Fehler, M.C., 2002b. Relocation of induced micro-earthquakes at the Soultz geothermal reservoir using automated, high-precision repicking. *Pure Appl. Geophys.* 159, 563–596.
- Rubin, A., Gillard, D., Got, J., 1998. A reinterpretation of seismicity associated with the January 1983 dike intrusion at Kilauea volcano, Hawaii. *J. Geophys. Res.* 103, 10003–10015.
- Shearer, P.M., 1997. Improving local earthquake locations using the L1 norm and waveform cross correlation: Application to the Whittier Narrows, California, aftershock sequence. *J. Geophys. Res.* 102, 8269–8283.
- Shearer, P.M., 1998. Evidence from a cluster of small earthquakes for a fault at 18 km depth beneath Oak Ridge, Southern California. *Bull. Seismol. Soc. Am.* 88, 1327–1336.
- Thurber, C.H., 1987. Seismic structure and tectonics of Kilauea volcano, Hawaii. Decker, R.W., Wright, T.L., Stauffer, P.H. (Eds.), *Volcanism in Hawaii*. U.S. Geol. Surv. Prof. Pap. 1350, pp. 919–934.
- Thurber, C., Eberhart-Phillips, D., 1999. Local earthquake tomography with flexible gridding. *Comp. Geosci.* 25, 809–818.
- VanDecar, J.C., Crosson, R.S., 1990. Determination of teleseismic relative phase arrival times using multi-channel cross-correlation and least squares. *Bull. Seismol. Soc. Am.* 80, 150–159.
- Zollo, A., Lomax, A., Capuano, P., Virieux, J., 2001. Precise earthquake location under Somma–Vesuvius volcano using a new three-dimensional velocity model. *Geophys. J. Int.* 146, 313–331.